HARD X-RAY AND METRIC/DECIMETRIC RADIO OBSERVATIONS OF THE 20 FEBRUARY 2002 SOLAR FLARE

N. VILMER[1], S. KRUCKER[2], R. P. LIN[2] and the RHESSI TEAM
[1]*LESIA, Observatoire de Paris, 92195- Meudon-Cedex, France*
[2]*Space Sciences Laboratory, University of California, Berkeley, CA-94720, U.S.A.*

(Received 8 August 2002; accepted 6 September 2002)

Abstract. The GOES C7.5 flare on 20 February 2002 at 11:07 UT is one of the first solar flares observed by RHESSI at X-ray wavelengths. It was simultaneously observed at metric/decimetric wavelengths by the Nançay radioheliograph (NRH) which provided images of the flare between 450 and 150 MHz. We present a first comparison of the hard X-ray images observed with RHESSI and of the radio emission sites observed by the NRH. This first analysis shows that: (1) there is a close occurrence between the production of the HXR-radiating most energetic electrons and the injection of radio-emitting non-thermal electrons at all heights in the corona, (2) modifications with time in the pattern of the HXR sources above 25 keV and of the decimetric radio sources at 410 MHz are observed occurring on similar time periods, (3) in the late phase of the most energetic HXR peak, a weak radio source is observed at high frequencies, overlying the EUV magnetic loops seen in the vicinity of the X-ray flaring sites above 12 keV. These preliminary results illustrate the potential of combining RHESSI and NRH images for the study of electron acceleration and transport in flares.

1. Introduction

Complementary observations of the hard X-ray (HXR) emitting electrons detected with RHESSI are provided by the radio emission produced in the whole frequency range from a few tens of GHz to a few MHz (see, e.g., Bastian, Benz, and Gary, 1998; White, 1999; Vilmer and Trottet, 1997; Vilmer and MacKinnon, 2002, for reviews of previous multiwavelengths observations of flares). These combined measurements allow to analyse the signature of non-thermal electrons in a whole range of coronal heights. While HXR and centimeter/millimeter wave emissions are the most direct diagnostic of the energetic electrons (see, e.g., Bastian, 1999; Nishio *et al.*, 1999; Lee, Gary, and Shibasaki, 2000; Lee and Gary, 2000), the coherent plasma radiations such as the ones emitted in the metric/decimetric domain at greater coronal heights (10^4-10^5 km) represent one of the most sensitive diagnostics of energetic electrons (a few tens of keV) injected in the corona from the flare site. In this paper, we shall focus on the radio observations in this frequency range.

It has been shown in many studies (see, e.g., Trottet, 1994; Vilmer and Trottet, 1997, for reviews) that multiwavelength studies provide a comprehensive approach to understanding particle acceleration and transport in solar flares. Several studies

Solar Physics **210:** 261–272, 2002.

have been previously performed combining hard X-ray/γ-ray spectral measurements with metric/decimetric radio imaging observations (e.g., Raoult *et al.*, 1985; Chupp *et al.*, 1993; Trottet *et al.*, 1994, 1998). They indicate that HXR and radio emissions arise from electrons produced in a common acceleration site and injected respectively in low-height magnetic structures where they produce X-rays and in larger scale, higher magnetic features where they emit decimetric and metric radiations. Many of these observations have also shown that in the course of the flare various large scale coronal structures are successively and/or simultaneously the sites of non-thermal electron radiation. The spectral characteristics of the flare energetic electrons as deduced from HXR observations evolve with time in close temporal association of the 'activation' of these large-scale magnetic structures in which radio emission is produced (Raoult *et al.*, 1985; Chupp *et al.*, 1993; Trottet *et al.*, 1994, 1998; Raulin *et al.*, 2000). It was thus suggested that the electron spectral variability may be linked to the magnetic configuration in which particles are produced. Such variations of HXR emitting electron spectra are also found to correspond to stepwise changes of metric/decimetric spectra (e.g., Trottet *et al.*, 1998). All these previous studies had been performed for flares for which there were either no HXR images or no 2D radio images in the decimetric/metric domains. Such a combination of HXR and radio 2D images was used so far only for the analysis of narrowband decimetric spikes (Benz, Saint-Hilaire, and Vilmer, 2002). The evolution with time of the associated HXR and radio emitting sites was however not investigated. Further probing the link between spectral and spatial variability at all scales is thus a major topic for HXR and possibly γ-ray imaging observations from RHESSI in combination with spatially and spectrally resolved observations in the whole radio domain.

In this paper, we present a first comparison of spatially resolved HXR and decimetric observations obtained for one of the first flares observed with RHESSI and we investigate the evolution in time and space of the pattern of small and large scale magnetic structures traced by the energetic electrons.

2. Instrumentation

The HXR and decimetric observations were obtained respectively by the RHESSI instrument (Lin *et al.*, 2002) and by the Nançay radioheliograph (Kerdraon and Delouis, 1996). At the time of the observations, the RHESSI instrument was operated with the thin shutters in front of the detectors thus cutting out the lowest energy photons (from ~ 3 to ~ 6 keV). The 2D imaging radioheliograph in Nançay provided observations at 432 MHz, 410 MHz, 327 MHz, 236 MHz, and 164 MHz. In the present study, only the highest frequency images are shown.

The radio spectra in the 150–550 MHz frequency range and in the 1–14 MHz range were obtained respectively by the *Phoenix-2* spectrometer operated by the ETH Zürich (Messmer, Benz, and Monstein, 1999) and by the WAVES experiment

aboard the WIND spacecraft (Bougeret *et al.*, 1995). EUV images provided at 195 Å by the Extreme Ultraviolet Imaging Telescope (EIT) aboard SOHO (Delaboudinière *et al.*, 1995) are also used to provide complementary information on the context in which the flare occurred.

3. Observations

3.1. Temporal evolution of the flare at X-ray and metric/decimetric wavelengths

The 20 February 2002 GOES C7.5 flare at 11:07 UT occurred in NOAA region 9825 (N16 W80). It is one of the first solar flares observed by RHESSI at X-ray wavelengths. The flare was seen from the HXR domain (up to around 100 keV) down to the hectometric radio domain. It was indeed simultaneously observed at metric/decimetric wavelengths by the Nançay radioheliograph (NRH) which provided images at five frequencies between 450 and 150 MHz and by the Phoenix-2 spectrometer which provided spectra in the same frequency domain. The WAVES experiment aboard the WIND spacecraft provided observations of the radio emission in the 1–14 MHz bands from electron beams injected in the high corona in association with the flare.

Figure 1 shows the time evolution of the counts (not background subtracted) in 4 energy bands (6–12, 12–24, 24–50, 50–100 keV) and of the X-ray spectrograms (background subtracted) from ~ 3 keV to $\sim$ 200 keV measured by RHESSI, together with the radio spectrum observed by *Phoenix-2* in the 150–550 MHz frequency range, the time evolution of the radio flux density at 164 MHz, 236 MHz, 327 MHZ, 408 MHZ , 432 MHz measured with the NRH and the radio spectrum from WIND/WAVES in the 1–14 MHz band.

For these observations thin shutters were placed in front of the RHESSI detectors leading to a decrease in the efficiency for measuring the lowest energy photons. Above 6 keV, the flare started at $\sim$11:04 UT and lasted until after 11:15 UT (Figure 1). The X-ray emission observed with RHESSI extends to energies of ~ 100 keV during a shorter time interval during the flare (~ 40 s around 11:06:20 UT). Although weak radio decimetric/metric emission is observed in the early phase of the flare (i.e., from the start of the X-ray emission in the 10 keV range), there is shortly after 11:06 UT a simultaneous sudden and strong increase of the HXR emission observed up to 100 keV and of the metric/decimetric radio flux. At this time, the radio emission is clearly seen in the metric/decimetric domain starting with groups of fast frequency drifting bursts. Although intense meter wavelength emission is observed, the emission at decimeter wavelengths (i.e., around 300 to 400 MHz) consists of fainter bursts of short bandwidth (see Figure 1). The simultaneous start of intense HXR and metric radio emissions is consistent with the results of previous studies (e.g., Benz *et al.*, 1983; Raoult *et al.*,

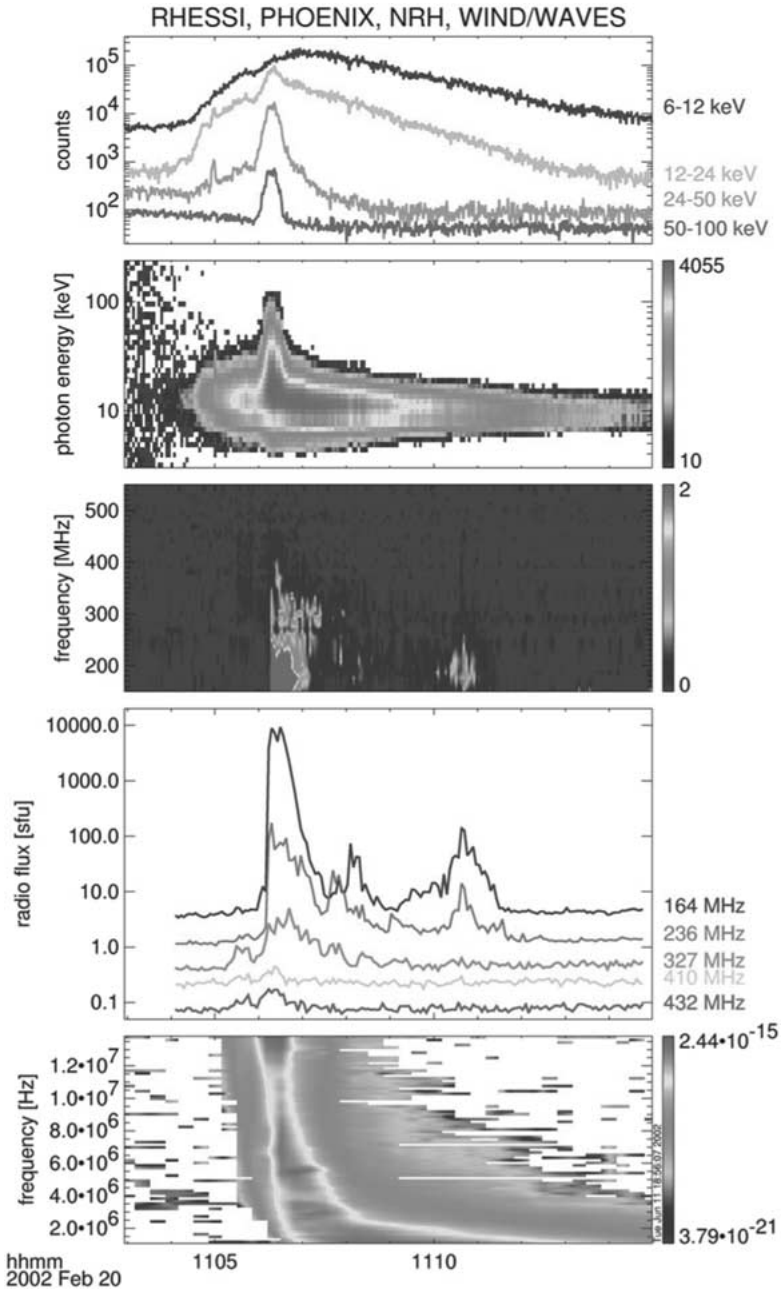

Figure 1. Top to bottom: time evolution of the X-ray RHESSI counts accumulated over 1 s in 4 energy channels between 6 keV and 100 keV (the background is not subtracted); RHESSI X-ray spectrogram showing the evolution with time and photon energy of the X-ray emission; decimetric/metric radio spectrum observed between 550 MHz and 150 MHz by *Phoenix-2* (ETH Zürich); decimetric/metric radio flux observed at 5 frequencies (integration time of 4 s) by the Nançay radioheliograph (NRH). The observed fluxes are respectively divided by: 1 (164 MHz), 5 (236 MHZ), 15 (327 MHz), 75 (410 MHz) and 150 (432 MHz); hectometric radio emission observed by the WIND/WAVES experiment. For color versions of this and other figures, see the CD-ROM.

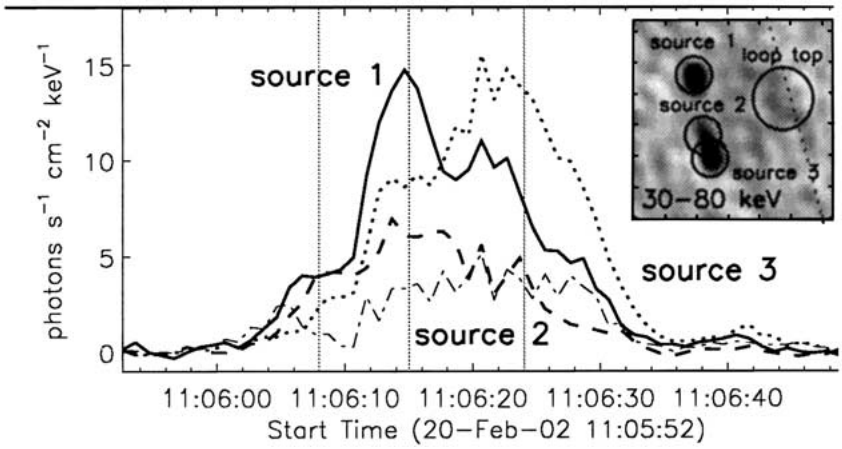

Figure 2. Temporal evolution of the different HXR sources observed at 30–80 keV at a resolution below 4″ (adapted from Krucker and Lin, 2002); source 1 (*solid line*), source 2 (*dashed line*), source 3 (*dotted line*), loop top (*dashed-dotted line*).

1985; Trottet *et al.*, 1998; Raulin *et al.*; 2000). The duration of the strongest part of the metric/decimetric radio emission is also found to be similar to the one of the HXR peak above 50 keV. As seen from Figure 1, the radio emission below 12 MHz (i.e., arising from electron beams injected in the high corona) also starts together with the sudden increase of the HXR flux at energies above 50 keV. This shows the link between the injection of electron beams towards the high corona and towards the HXR emitting sites.

3.2. HXR AND DECIMETRIC IMAGING OBSERVATIONS

3.2.1. *In the Main HXR Burst*

The imaging spectroscopic capabilities of RHESSI are demonstrated for this flare in Krucker and Lin (2002). At energies above 30 keV and a spatial resolution below 4″, the emission comes primarily from 3 compact sources (Figure 2): source 1 to the north, source 3 to the south and a weaker source 2 in between but much closer to source 3. Figure 2 also shows the loop top source discussed in more detail in Sui *et al.* (2002). The time evolution of the photon flux in the different sources is displayed in Figure 2. While a first HXR peak at ∼11:06:15 UT is observed coming primarily from the northern component (source 1), a second peak of similar amplitude is observed peaking shortly after 11:06:20 UT originating from the southernmost component (source 3).

The goal of this paper is not to describe in detail the evolution of the X-ray images in different energy bands but to present a first comparison of the time evolution of the radio and of the HXR emitting sites from non-thermal electrons. We shall furthermore focus on the images provided in the highest frequency band by the NRH, since the emissions around 400–300 MHz are more likely to be

produced close to the energy release and acceleration sites of X-ray producing electrons (e.g., Benz and Aschwanden, 1991). Indeed, studies based on frequency drifts of decimetric type III bursts or on starting frequencies of pairs of opposite drifting bursts (commonly observed between 300 MHz and 1 GHz) indicate that electron beam acceleration responsible for both downward moving HXR producing electrons and upward radio emitting electrons arise from a medium with densities ranging from 10^9 to 10^{10} cm^{-3} (Benz and Aschwanden, 1991; Aschwanden *et al.*, 1995).

Figures 3 and 4 show combined images of the X-ray emission in the 25–40 keV range and of the decimetric radio emission at 410 MHz superposed on an EIT difference image measured at 195 Å shortly after the HXR flare. While Figure 3 corresponds to a time where X-ray sources 1 and 3 are of equal importance (see Figure 2), Figure 4 corresponds to a time where the southernmost source 3 is predominant. The radio emission sites in both Figures 3 and 4 present a double component. As seen from these figures, the modification of the HXR morphology between the two images correspond to a noticeable change of the relative brightness of the two components of the radio sources at 410 MHz. This shows a causal relationship between the radio and HXR emitting sites which can be attributed to variations in the energy release and electron injection sites. Such variations of the radio emission sources in the development of X-ray flares has been described already in different papers (see, e.g., Chupp *et al.*, 1993; Trottet *et al.*, 1994, 1998). Although it had been suggested that such modifications in the radio emitting sites could be related to variations on the same time period in the morphology of the X-ray emitting sources, a direct comparison such as the one presented here had not been achieved so far.

3.2.2. *In the Late Phase of the HXR Peak*

In the previous section, a comparison of the X-ray and high frequency radio emitting sources was done for two specific time intervals. Figure 5 shows a time series of radio images at 410 and 327 MHz each integrated over 4 s. The field of view is the same for both frequencies and the brightness levels in each image are normalized to the maximum of the image. Figure 5 shows that during most of the HXR main peak (i.e., from 11:06:05 to 11:06:29 UT), the radio emission arises at the two frequencies from two close components with variable relative intensities. At 410 MHz the outermost component of the radio sources is predominant compared to the innermost one (as in Figure 4) from 11:06:21 to 11:06:29 UT (see Figure 5 top), i.e., at the time when the southernmost HXR source (source 3) is the strongest component of the HXR emission.

Figure 5 shows that a radio source is seen (both at 410 MHz and 327 MHz) for a few images around 11:06:33 UT (i.e., in the late phase of the main HXR burst), closest to the limb and to the X-ray flare site. Figure 6 shows combined images at 11:06:33 UT of the X-ray emission in the 12–18 keV range and of the decimetric radio emission observed at 410 MHz superposed on the EIT im-

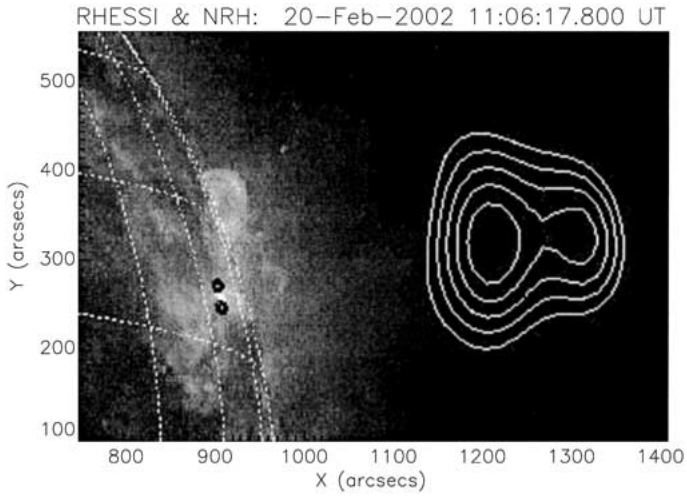

Figure 3. RHESSI iso-contours (*black*) (40, 60, 80% of the maximum) at 25–40 keV and NRH contours at 410 MHz (*white*) (50, 60, 70, 80, 90%) observed at 11:06:17.800 at the time when similar flux is radiated from sources 1 and 3 (see text). The RHESSI and NRH contours are superposed on the closest EIT image obtained at 11:12 UT. The RHESSI images are obtained using grids 3 to 9 giving a resolution of $7''$.

age obtained shortly after the flare. The X-ray source at 12–18 keV presents a double component, similar to the one observed at higher energies earlier in the flare. At 11:06:33 UT, the northern component is predominant. At 410 MHz, the emission comes predominantly from a new emitting site very close to the limb. The innermost radio component observed previously at the time of the main HXR burst (Figure 4) is still observed, even if its flux has largely decreased. The new radio source is observed in the high frequency part of the NRH observing domain (i.e., 432 MHz, 410 MHz, and 327 MHz) and corresponds to a weak flux of less than 10 s.f.u. It overlays magnetic loops seen with EIT in the close vicinity of the flaring active region. Around 11:06:33 UT, there is still a significant production of non-thermal X-ray emission between 10 and 30 keV (although with a steeper spectrum than during the main phase) (see Figure 1). A detailed discussion of the origin of the radio source overlying the EIT loops is beyond the scope of this paper which presents early science results from RHESSI. A preliminary analysis of the RHESSI spectra shows however that non-thermal electrons between 10 and 30 keV are detected during that period.

4. Summary of the Observations and Discussion

This paper presents the results of the preliminary analysis of the 20 February 2002 solar flare at 11:06 UT based on the first comparison of RHESSI and NRH images. The results are summarized below:

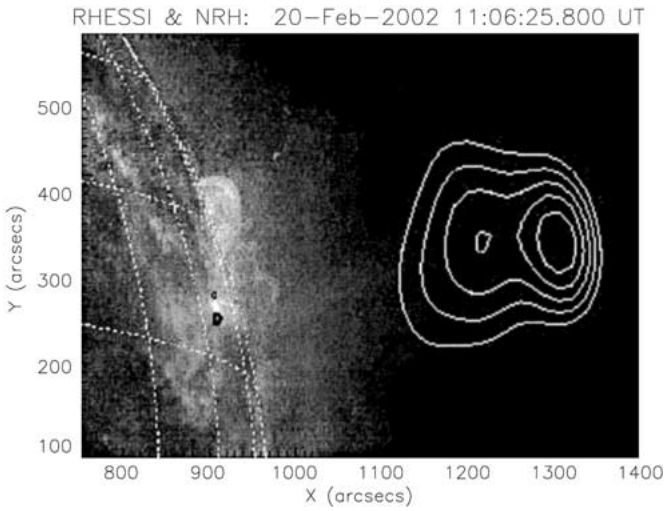

Figure 4. Same as Figure 3 at 11:06:25.800 at a time where the southernmost source 3 is predominant (see text). The change of the relative brightness of the two radio components has to be noted.

– Although weak radio decimetric/metric emission is observed in the early phase of the flare in the 10 keV range, intense metric emission starts together with the most energetic X-ray peak observed up to almost 100 keV. This is in good agreement with previous combined observations of spatially unresolved HXR observations and of metric/decimetric observations (e.g., Benz *et al.*, 1983, Raoult *et al.*, 1985; Trottet *et al.*, 1998). The duration of the strongest part of the radio emission in the whole decimetric/metric range is similar to the one of the HXR peak above 50 keV, suggesting as in the previously quoted works a common acceleration site with simultaneous injection of electrons both in low-lying magnetic features where they produce X-rays and in larger scale and higher magnetic structures where radio emission is produced.

– The main results lie in the first comparison of the variations on a few seconds time scale of HXR images above 25 keV and of decimetric radio images. Modifications of the X-ray sources above 25 keV (Figures 3 and 4) are associated with coincident changes in the morphology of the decimetric radio sources. Such changes of the HXR and radio emitting sites occurring on a similar time period had been suggested previously (e.g., Trottet, 1986, 1994; Vilmer and Trottet, 1997) based on several multiwavelength studies combining HXR spectral measurements with metric/decimetric radio imaging observations. Direct comparisons of HXR and radio images obtained on a few seconds time resolution could not be, however, performed. The present observations thus support the previous suggestion of common acceleration/injection sites for HXR and decimetric/metric emitting electrons. Indeed, variations in the HXR and decimetric emitting sites observed over the same time period show that both emissions are closely related to the energy release sites and to their variations during the flare. The link between the X-ray and radio

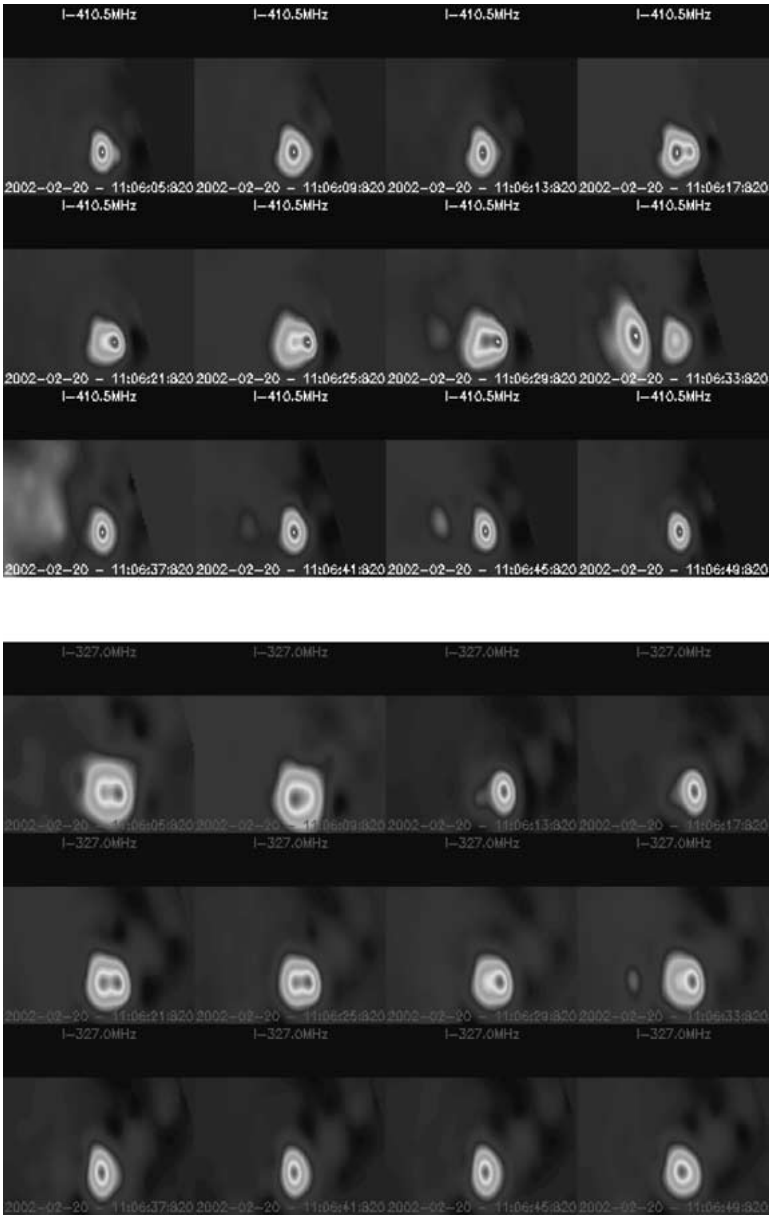

Figure 5. Time series of radio images integrated over 4 seconds at 410 (*top*) and 327 MHz (*bottom*) and observed by the NRH. During the time of the HXR peak above 50 keV, the radio sources consist of two close components with variable relative intensities (see also Figures 3 and 4) The appearance of a weak transient radio source closest to the limb and to the X-ray source can also be noted (see Figure 6). (NB: each image is normalized to its maximum.)

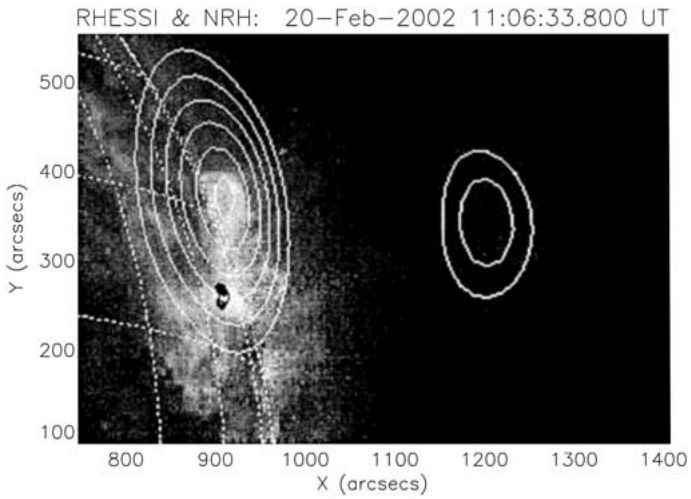

Figure 6. RHESSI iso-contours (*black*) (40, 60, 80%) at 12−18 keV and NRH contours (*white*) at 410 MHz (50, 60, 70, 80, 90%) at 11:06:33.800 UT superposed on the same EIT image at 11:12:10:489 UT.

sources and their evolution is, however, not easy to understand in detail without the knowledge of the magnetic connections between the emitting sites. Noticeable changes in the accelerated electron spectra deduced from HXR spectral analysis have been reported in close connection with the changes of the spatial distribution of the electron emitting sites at radio wavelengths (e.g., Chupp *et al.*, 1993; Trottet *et al.*, 1994, 1998; Raulin *et al.*, 2000) similar to the ones shown here in Figures 3 and 4. Spectral variations of the different X-ray sources in this event are presented elsewhere (Krucker and Lin, 2002). A detailed temporal comparison of the spectral evolution of the energetic electrons and of the variations of the pattern of the radio emitting sites is beyond the scope of this preliminary analysis and will be analysed later.

A weak radio source is observed at high frequencies in the late phase of the main HXR burst, overlying EIT magnetic loops and in close proximity of the X-ray flaring sites above 12 keV. The emission comes predominantly from the northern component of the X-ray source. The origin of the weak radio source has not been investigated in detail in this paper and additional work is needed in the future. The observations however suggest that this emission could be linked to the production of non-thermal electrons above 12 keV predominantly observed in the northern part of the flaring active region and subsequently injected towards magnetic field lines overlying the magnetic loops seen at the limb by EIT.

As a conclusion, the present results based on a preliminary comparison between HXR and decimetric/metric images demonstrate the potential of combined RHESSI and NRH observations to understand the properties of electron acceleration/injection and radiation in magnetic structures of all scales. Such comparisons

will be performed on many other and more intense flares than this moderate one giving additional possibilities to achieve imaging spectroscopy at higher energies and detailed comparisons between high energy HXR sources and radio emitting sites. The possibility of imaging radio emitting electrons low in the corona (i.e., in the high frequency range of the NRH band) is quite promising in terms of comparison with X-ray emitting sites, since these emissions lie relatively close to acceleration sites. This also demonstrates the potential interest of imaging radio emissions from non-thermal electrons at even higher frequencies (as planned, e.g., by the FASR project) to better image the acceleration sites of the electrons which are responsible for HXR emission and which are now observed with unprecedented imaging-spectroscopy capabilities with RHESSI.

Acknowledgements

N. Vilmer acknowledges support from the Centre National d'Etudes Spatiales on the RHESSI project. The Nançay Radio Observatory is funded by the French Ministry of Education, the CNRS and the Région Centre. The authors would like to thank Dr T. Bastian for valuable comments on the first version of the manuscript. They are also grateful to Dr H. Hudson for his useful comments.

References

Aschwanden, M. J., Benz, A. O., Dennis, B. R., and Schwartz, R. A.: 1995, *Astrophys. J.* **455**, 347.

Bastian, T.: 1999, in T. S. Bastian, N. Gopalswamy and K. Shibasaki (eds.), *Proceedings of the Nobeyama Symposium, NRO Report* **479**, 211.

Bastian, T., Benz, A. O., and Gary, D. E.: 1998, *Ann. Rev. Astron. Astrophys.* **36**, 131.

Benz, A. O. and Aschwanden, M.: 1991, in Z. Švestka, B. V. Jackson, and M. E. Machado (eds.), *Eruptive Solar Flares, Lecture Notes in Physics* **399**, 106.

Benz, A. O., Saint-Hilaire, P., and Vilmer, N.: 2002, *Astron. Astrophys.* **388**, 363.

Benz, A. O., Barrow, C. H., Dennis, B. R., Pick, M., Raoult, A., and Simnett, G.: 1983, *Solar Phys.* **83**, 267.

Bougeret, J. L. *et al.*: 1995, *Space Sci. Rev.* **71**, 231.

Chupp, E. L., Trottet, G., Marschhäuser H. *et al.*: 1993, *Astron. Astrophys.* **275**, 602.

Delaboudinière, J. P., Artzner, G. E., Brunaud, J. *et al.* : 1995, *Solar Phys.* **162**, 291.

Kerdraon, A. and Delouis, J. M.: 1997, in G. Trottet (ed.), *Coronal Physics from Radio and Space Observations, Lecture Notes in Physics* **483**, 192.

Krucker, S. and Lin, R. P.: 2002, *Solar Phys.*, this volume.

Lee, J. and Gary, D. E.: 2000, *Astrophys. J.* **543**, 457.

Lee, J., Gary, K., and Shibasaki, K.: 2000, *Astrophys. J.* **531**, 1109.

Lin, R. P. *et al.*: 2002, *Solar Phys.*, this volume.

Messmer, P., Benz, A. O., and Monstein, C.: 1999, *Solar Phys.* **187**, 335.

Nishio, M., Kosugi, K., Yaji, K. *et al.*, 1999, in T. S. Bastian, N. Gopalswamy and K. Shibasaki (eds.), *Proceedings of the Nobeyama Symposium, NRO Report* **479**, 235.

Raoult, A., Pick, M., Dennis, B. R., *et al.*: 1985, *Astrophys. J.* **299**, 1027.

Raulin, J. P., Vilmer, N., Trottet, G. *et al.*: 2000, *Astron. Astrophys.* **355**, 355.

Sui, L., Holman, G. D., Dennis, B. R., Krucker, S., Schwartz, R. A., and Tolbert, K.: 2002, *Solar Phys.*, this volume.
Trottet, G.: 1986, *Solar Phys.* **104**, 145.
Trottet, G: 1994, *Space Sci. Rev.* **68**, 149.
Trottet, G., Chupp, E. L., Marschhaüser, H. *et al.* : 1994, *Astron. Astrophys.* **288**, 647.
Trottet, G., Vilmer, N., Barat, C. *et al.*: 1998, *Astron. Astrophys.* **334**, 1099.
Vilmer, N. and Trottet, G.: 1997, in G. Trottet (ed.), *Coronal Physics from Radio and Space Observations, Lecture Notes in Physics* **483**, 28.
Vilmer, N. and MacKinnon, A. L.: 2002, in K. L. Klein (ed.), *Lecture Notes in Physics*, in press.
White, S. M.: 1999, in T. S. Bastian, N. Gopalswamy, and K. Shibasaki (eds.), *Proceedings of the Nobeyama Symposium, NRO Report* **479**, 223.